The Journal of Chemical Physics

Analysis of chemical bonding of the ground and low-lying states of Mo_2 and of Mo_2Cl_x complexes, x = 2–10

Cite as: J. Chem. Phys. **157**, 054302 (2022); https://doi.org/10.1063/5.0091907
Submitted: 18 March 2022 • Accepted: 04 July 2022 • Accepted Manuscript Online: 04 July 2022 • Published Online: 03 August 2022

Teo Depastas, Alexandros Androutsopoulos and Demeter Tzeli

The Journal of Chemical Physics ARTICLE scitation.org/journal/jcp

Analysis of chemical bonding of the ground and low-lying states of Mo_2 and of Mo_2Cl_x complexes, x = 2–10

Cite as: J. Chem. Phys. 157, 054302 (2022); doi: 10.1063/5.0091907
Submitted: 18 March 2022 • Accepted: 4 July 2022 •
Published Online: 3 August 2022

Teo Depastas,[1] Alexandros Androutsopoulos,[1] and Demeter Tzeli[1,2,a)]

AFFILIATIONS

[1] Laboratory of Physical Chemistry, Department of Chemistry, National and Kapodistrian University of Athens, Panepistimiopolis Zografou, Athens 157 84, Greece
[2] Theoretical and Physical Chemistry Institute, National Hellenic Research Foundation, 48 Vassileos Constantinou Ave., Athens 116 35, Greece

Note: This paper is part of the JCP Special Topic on Nature of the Chemical Bond.
[a)]**Author to whom correspondence should be addressed:** tzeli@chem.uoa.gr. **Tel.:** +30-210-727-4307

ABSTRACT

In this study, we perform accurate calculations via multireference configuration interaction and coupled cluster methodologies on the dimolybdenum molecule in conjunction with complete series of correlation and weighted core correlation consistent basis sets up to quintuple size. The bonding, the dissociation energies, and the spectroscopic parameters of the seven states that correlate with the ground state products are calculated. The ground state has a sextuple chemical bond, and each of the calculated excited states has one less bond than the previous state. The calculated values for the ground $X^1\Sigma_g^+$ state of Mo_2 have been extrapolated to the complete basis set limits. Our final values, r_e = 1.9324 Å and D_e (D_0) = 4.502 ± 0.007(4.471 ± 0.009) eV, are in excellent agreement with the experimental values of r_e = 1.929, 1.938(9) Å and D_0 = 4.476(10) eV. Mo_2 in the $^{13}\Sigma_g^+$ state is a weakly bound dimer, forming $5s\cdots5p_z$ bonds, with D_e = 0.120 eV at r_e = 3.53 Å. All calculated excited states (except $^{13}\Sigma_g^+$) have a highly multireference character (C_0 = 0.25–0.55). The ordering of the molecular bonding orbitals changes as the spin is increased from quintet to septet state resulting in a change in energy separation $\Delta_{S,S-1}$ of the calculated states. The quite low bond dissociation energy of the ground state is due to the splitting of the molecular bonding orbitals in two groups differing in energy by ~3 eV. Finally, the bond breaking of Mo_2, as the multiplicity of spin is increased, is analyzed in parallel with the Mo–Mo bond breaking in a series of Mo_2Cl_x complexes when x is increased. Physical insight into the nature of the sextuple bond and its low dissociation energy is provided.

I. INTRODUCTION

The chemical bond is one of the most fundamental and basic pillars of Chemistry.[1–3] Many books of quantum chemistry start with the famous phrase of Mulliken "*I believe the chemical bond is not so simple as some people seem to think.*"[2] Since 1960, many research articles have been published focusing on the chemical bonding of many molecular systems, while it remains a favorite topic and attracts the interest and the attention of chemists. This happens because the comprehension of chemical bonds results in qualitatively predicting and understanding of the mechanism and the outcome of chemical processes that lead from separated atoms or molecular fragments to energetically stabilized molecular structures.[4–7]

Covalent chemical bonding is central to the understanding of chemical structures and reactions. However, even though its formation is arguably the most fundamental chemical process, its physical origin has remained obscure to most chemists, and it is still the subject of debate, even today, when accurate quantitative molecular electronic structure calculations of ever-increasing complexity have become widely available.[8] Since 1962, Ruedenberg and co-workers[6–22] began to develop analyses aimed at discerning the physical relationships that are embedded in the rigorous framework of molecular electronic wave functions and binding energies. They

have studied a series of small molecules including homoatomic and heteroatomic diatomics and cations.[6–22] They showed that the critical bonding contribution results from the lowering of the kinetic energy through inter-atomic electron delocalization, a conclusion that agrees with the inference that Hellmann had drawn from different considerations.[8]

The order of a chemical bond, i.e., the multiplicity of a chemical bond, is the number of electron pairs that occupy the region between the two bonded atoms in bonding molecular orbitals minus the number of electron pairs in the antibonding molecular orbitals. Multiple bonds up to triple bonds have been known since the 19th century.[23] Triple bonds are quite common in organic compounds and in some common molecules, such as N_2 and CO. In 1964, Cotton *et al.* introduced, for the first time, the idea of a quadruple bond between two transition-metal atoms for the crystal structure of $K_2[Re_2Cl_8]\cdot 2H_2O$.[24] Since then, quadruple bonds have been reported on a few other occasions. It is interesting that they have been suggested for diatomic molecules of main group elements, i.e., C_2, CN^+, BN, and CB^-.[25] Specifically, the exact multiplicity of the bond of the C_2 molecule has been investigated thoroughly.[25–32] Recently, quadruple bonds have been reported for the ground states and low-lying excited states of diatomic molecules containing main group elements and transition metals of the second row, i.e., RhB,[33,34] TcN,[34] RuC,[34] and PdBe,[34] and their anions.[35] The requirements for the occurrence of such bonds in molecular systems have been reported.[34,35] Quintuple bonding has been reported between two Cr(I) centers in a stable compound,[36] while sextuple bonding, which is regarded as the maximum multiple bonds,[37] has been proposed for the homonuclear diatomic transition metals of the VIB group, specifically, Cr_2, Mo_2, and W_2.[37] An in-depth discussion on the bond energies and multiple bonding of group 4 metallic homo- and heteronuclear dimers is presented in Ref. 38.

Experimentally, the Mo_2 molecule was synthesized at low temperature using cryophotoclustering techniques in 1977,[39] while its absorption spectrum was measured.[39,40] The following year, its thermodynamic properties were studied via high-temperature mass spectrometry, and the first experimental dissociation energy was obtained, $D_0 = 4.2 \pm 0.2$ eV.[41] In 1978, both the absorption and emission spectra of Mo_2 were investigated using flash photolysis of the $Mo(CO)_6$ molecule.[42] Bond distances and vibrational frequencies were measured via time resolved fluorescence spectroscopy,[43] photoionization spectroscopy,[44,45] and optical spectroscopy using a Fourier transform spectrometer (2001).[46] The r_e bond length was measured at 1.940 ± 0.009, while its dissociation energy was found at $D_0 = 4.476(10)$ eV[45] (see Table I). Finally, some low-lying

TABLE I. Previous theoretical and experimental data on the ground state $X^1\Sigma_g^+$ of Mo_2; bond length r_e (Å), dissociation energies D_e and D_0 (eV), and vibrational frequency and anharmonic corrections ω_e and $\omega_e\chi_e$ (cm^{-1}).

Methodology	References	r_e	D_e	D_0	ω_e	$\omega_e\chi_e$
SCF-$X\alpha$-SW	40	2.10				
High-temperature mass spectrometry	41			4.18(0.21)		
Flash photolysis	42	1.929		4.11(0.65)	477.1	1.51
Time resolved fluorescence spectroscopy	43	1.90(2)			475.7(4.5)	
Photoionization spectroscopy	44	1.938(9)				
Photoionization spectroscopy	45			4.476(10)		
Optical spectroscopy	46					
Spin polarized cellular multiple scattering	54	2.1481	4.10			
MCSCF(APSG)/[8s4p3d]	48	2.10	4.4566			
SCF-$X\alpha$-SW	49		0.693			
CIS(CID)/[12s5d4d]	52	2.01(1.90)		0.86(2.16)	388(676)	
MCSCF(APCG)/[12s5d4d]	52	2.02	3.10		392	
GVB-vdw/dz+f	51	1.97	1.41		455	
LDA/[15s15p14d]	57	1.8212	4.2951	4.2645	493.58	
B3LYP/SDD	46	1.965			533.5	
PW91/plane-waves	60	1.80	5.08			
PBE/tz+polarization	63	2.066	3.38		439	
SC-NEVPT2/ANO-RCC[21p13d6f4g2h|857p5d3f2g]	65	1.9198	5.055		506.09	1.67
SC-NEVPT3/[21p13d6f4g2h|857p5d3f2g]	65	1.9500	3.9868		461.54	1.64
PC-NEVPT2/[21p13d6f4g2h|857p5d3f2g]	65	1.9198	5.1163		504.50	1.63
PW91/DND	58	1.98	3.00		523	
CASPT2/ECP-[6s5p3d]	64	2.09	2.14		358	
PNOF5/ECP-[6s5p3d]	64	2.10	3.26		368	
CCSD(T)[PBE]/cc-pVTZ-PP	59	1.932[1.925]				
DMC/SDSJ/cc-pV5Z-PP	66	1.93		2.92(3)		
DMC/MDSJ/cc-pV5Z-PP	66	1.93		3.56(3)		

electronic states of Mo_2 have been observed in matrix isolation fluorescence studies. Phosphorescence[46] was observed from a state lying at approximately T_0 = 7977.6 cm^{-1} above the ground state with an estimated vibrational frequency of 393.7 cm^{-1}. This matches fairly nicely with our calculated $^3\Sigma_u^+$ state, see below. Moreover, another excited state lying at T_0 = 13 747 cm^{-1} was found to phosphoresce to the ground state.[43,47] This is lying in the right range to correspond to the $^5\Sigma_g^+$ state here, see below.

The first theoretical study on Mo_2 was published in 1977,[40] where the ground state of Mo_2 was calculated via extended Hückel[40] and SCF-Xa-SW.[40] In 1979, the ground state of Mo_2 was calculated initially by Wood *et al.*[48] via MCSCF calculations, by Norman and Ryan,[49] and by Bursten and Cotton[50] via SCF-Xa-SW calculations. Over the next few years, GVB,[51] ASPG,[52,53] CID,[52,53] and spin polarized cellular multiple scattering[54] calculations were carried out. The first calculations on this large, multi-electron molecule were very demanding tasks given the very poor computational resources, compared to the current ones. As a result, the calculated dissociation energies were not very good; they ranged from almost zero (Configuration Interaction Singles, CIS) to 9.35 (Self-Consistent Field, SCF)[52] eV depending on methodology. However, very interesting discussions, comments, and physical insights were obtained. In subsequent years, a variety of methodologies were employed for the calculation of the ground state, i.e., *ab initio* Green's function method,[55] extended Huckel method (SCMEH-MO),[56] density functional theory (DFT),[46,57–62] coupled cluster singles doubles triple [CCSD(T)],[59] CASPT2,[63] natural orbital functional theory (NOFT),[64] NEVPT2,[65] and quantum Monte Carlo methodology[66] (see Table I). As given in this table, the experimentally measured values of the bond dissociation energy (D_0) range from 4.11 ± 0.65 to 4.476 ± 0.10[45] eV, i.e., the range is rather narrow. On the contrary, the calculation of the corresponding theoretical dissociation energy is a demanding task, and this is the reason for the large range of the calculated values. In Table I, the evolution for the D_e calculations is observed. Regarding the bond length of the ground state, a large range of the calculated values is also observed, namely, the r_e value has been calculated from 1.80 to 2.10 Å. Thus, there is a need for benchmark theoretical calculations, where the dissociation energies and bond distances will be extrapolated to complete basis set limits.

In most published studies, the bond is regarded as a sextuple one, even though the bond dissociation energy is very low for this kind of bond. Additionally, the bonding of complexes of Mo_2, i.e., Mo_2H_6 and $Mo_2(NH_2)_6$,[67] $Mo_2[(CH_2)_2P(CH_3)_2]I_4$,[68] and $[Mo_2(\mu\text{-Li})\{\mu\text{-HC(N-2,6-Et}_2C_6H_3)_2\}_3]$,[69] have been studied and their Mo–Mo bonds have been regarded of orders 3, 4, and 5, respectively. Finally, it should be noted that there are also studies, where the bond multiplicity of the simple Mo_2 molecule is regarded as less than 6, i.e., 4.12.[70]

Comparing the homonuclear diatomic transition metals of the VIB group, Cr_2, Mo_2, and W_2, all forms sextuple bonds and present a $X^1\Sigma_g^+$ state as the ground one.[37,61] The sextuple bond in Cr_2 is very short, i.e., 1.68 Å,[61] while its bond dissociation energy is only 1.66 eV.[37] This is attributed to the fact that the 3d and 4s orbitals differ in size, i.e., the large 4s orbital generates a 4s–4s bond that is a longer bond length than the 3d–3d bonds. This unbalance weakens the 3d–3d bonds, while it makes the 4s–4s bond repulsive at equilibrium geometry.[37] The Mo_2 and W_2 molecules present quite similar bond distances and bond dissociation energies. Both quantities are larger than the corresponding values of Cr_2, i.e., the bond distances of Mo_2 and W_2 are 1.938(9)[44] and 1.9977 Å,[65] respectively, while their bond dissociation energies are 4.476(10)[45] and 4.511 eV[65] (5.55 ± 0.42 eV, estimated experimentally value),[71] respectively.

In this study, we perform high-level multireference configuration interaction and coupled cluster theoretical calculations on the dimolybdenum molecule. The bonding, the dissociation energies, and the spectroscopic parameters of the seven states that correlate with the ground state products are calculated. As far as we know, the excited states of Mo_2 have not been calculated before. Experimentally, the $A^1\Sigma_u^+$[44] excited state has been measured, where at least one Mo atom is excited. The sextuple bond breaking of Mo_2, as the multiplicity of spin is increased, and the corresponding Mo_2Cl_x complexes, as the number of complexed Cl is increased, are investigated in parallel, adding physical insight into the nature of the sextuple bond and its dissociation energy. We found that when the multiplicity of bonds changes from triple to quadruple, the average bonding energy is increased. Our data are in excellent agreement with the experimental data. In addition, it was found that the Mo_2 in the $^{13}\Sigma_g^+$ state is a weakly bound dimer.

II. COMPUTATIONAL DETAILS

A. Basis sets and methodology

Mo has a quasi-relativistic character due to its rather large nuclear charge, and as a result, the use of basis sets employing pseudopotentials for the inner electrons or Douglas–Kroll consistent basis sets is necessary. The ground and the six excited Λ-S states of Mo_2, which correlate with the atomic ground state products, are calculated via multireference configuration interaction and coupled cluster methodologies.

The correlation consistent basis sets, aug-cc-pV*n*Z-PP,[72] and the weighted core correlation consistent, aug-cc-pwCV*n*Z-PP,[72] n = D, T, Q, and 5 are used employing accurate core relativistic pseudo-potentials for the $1s^22s^22p^63s^23p^6$ electrons and treat the $4s^24p^6(5s4d)^6$ electrons of each Mo explicitly in the *ab initio* calculation, i.e., 28 electrons for Mo_2. Using the first basis set, the correlation of the $(5s4d)^6$ electrons is calculated, while the $4s^24p^6$ electrons are kept frozen. On the contrary, using the second group of basis set (wC), the correlation of all 28 electrons is computed. The contraction scheme of the largest basis set is up to (19s, 16p, 14d, 6f, 5g, 4h, 3i) → [10s, 10p, 9d, 6f, 5g, 4h, 3i]. Furthermore, scalar relativistic effects, i.e., mass–velocity and Darwin terms, are considered by the second and ninth order Douglas–Kroll–Hess (DKH2 and DKH9) approximation,[73] employing the aug-cc-pVTZ-DK and aug-cc-pwCVTZ-DK basis sets,[72] where the correlation of 2 × $[(5s4d)^6]$ and 2 × $[4s^24p^6(5s4d)^6]$, respectively, is calculated. The 36 inner electrons, 2 × $1s^22s^22p^63s^23p^6$, are kept frozen.

The potential energy curves (PECs) of the seven states correlated with the atomic ground state products are calculated via multireference methodology employing the aug-cc-pV*n*Z-PP basis set. At first, complete active space self-consistent field (CASSCF) calculations are carried out where 12 valence electrons are allotted to 12 valence orbitals, i.e., six (5s4d) of each Mo, and up to 95 391 CSFs are used. Then, the multireference configuration interaction

+ single + double excitations (MRCISD),[74] MRCISD+Q[75] where the Davidson correction (+Q) is included in MRCISD, methodology is applied. The size of the MRCISD spaces is up to 6.9×10^9 and it is reduced to about 4×10^7 CSFs after applying the internal contraction approximation (icMRCISD).[74]

Moreover, the X state is also calculated via the restricted coupled cluster + singles + doubles + perturbative triples RCCSD[T] methodology.[76] In addition, the C-RCCSD[T] methodology was used in conjunction with the wC basis sets, where the semi-valence $4s^2 4p^6$ electron are included in the correlated space. Note that, for the MoS molecule,[77] it was found that the perturbative inclusion of the triplets via C-RCCSD[T] was in excellent agreement with the experimental data[77] and slightly better than C-RCCSD(T); thus, the C-RCCSD[T] methods were used here. In addition, the potential energy curve (PEC) of $^{13}\Sigma_g^+$ state is computed at the RCCSD[T]/aug-cc-pwCVQZ-PP level. The single (t1) and the double (t2) amplitudes and the T1 and D1 diagnostic are checked. It is found that, in all calculations, the t1 and t2 amplitudes were very small. For the of $^1\Sigma_g^+$ state, t1 and t2 are smaller than 0.05 (only few are larger than 0.05), T1 < 0.06, and D1 < 0.1. For $^{13}\Sigma_g^+$ state, t_1 and t_2 are smaller than 0.05, T1 < 0.01, and D1 < 0.04. These small values of t1 and t2 amplitudes and of the T1 diagnostic indicate that the CC methodology is appropriate for the calculation of both $^1\Sigma_g^+$ and $^{13}\Sigma_g^+$ states. Furthermore, it should be noted that while the $^{13}\Sigma_g^+$ state is a single reference state, the main CAS configuration of the $^1\Sigma_g^+$ is 80%, i.e., it has a multi-reference character. However, recently, it has been reported that coupled cluster calculations including perturbative triples, CCSD(T), are quite accurate even with 77%.[78]

Finally, the bonding of the seven calculated states of the Mo_2 molecule is compared with the bonding of the Mo_2Cl_x complexes, where x = 2–10. The complexes are calculated at the DFT level, i.e., TPSSh[79]/aug-cc-pVTZ-PP. For the calculated structures, their frequencies are calculated to check if they are true minimum structures.

All multireference and coupled cluster calculations were carried out with the MOLPRO[80] suite of codes and DFT calculations with GAUSSIAN.[81]

B. Computation of spectroscopic constants

The PECs are fitted by polynomial functions of the form $E = \sum_{i=0}^{N} a_i r^i$, where N > 5 up to 12. The fitting procedure is accomplished via a python code, supplemented with the scipy library. The minimum of the curve corresponds to r_e and its curvature at equilibrium to $\omega_e = \frac{k^{1/2}}{2\pi c \mu^{1/2}}$, where $k = \frac{d^2E(r_e)}{dr^2}$ and μ is the reduced mass of $^{100}Mo_2$. The $(N-1)$th order minimization equation is solved through a Newton–Raphson code. The MRCISD+Q bond dissociation energy is calculated as D_e = E(20 Å) − E(r_e). The size-nonextensivity error is 0.034 eV. For the coupled cluster calculations, the D_e values have been obtained from the calculated energy of the separated atoms minus the energy calculated for the electronic state at its potential energy minimum. The anharmonicity constant is calculated as $\omega_e\chi_e \approx \frac{\omega_e^2}{4D_e}$ and the experimental dissociation energy as $D_0 \approx D_e - \frac{\omega_e}{2}$. The rotational constants are calculated by the relations $B_e = \frac{h}{8\pi^2 c \mu r_e^2}$ and $D_J = \frac{4B_e^3}{\omega_e^2}$.

C. Basis set limit and extrapolation schemes

The ground state, $X^1\Sigma_g^+$, is systematically studied by employing the C-RCCSD[T] method, in conjunction with a systematic sequence of weighted core correlation consistent Gaussian basis sets, i.e., aug-cc-pwCVnZ-PP, n = D, T, Q, and 5, where the semi-valence electrons, $4s^2 4p^6$ electrons, of Mo are also included in the valence space of the C-RCCSD[T] method. All calculated values, i.e., bond distances, dissociation energies, and other spectroscopic parameters, are calculated in a series of basis sets, and then, these obtained values are extrapolated using four extrapolated schemes to find the Complete Basis Set (CBS) limit. Specifically, the mixed Gaussian/exponential formula (1),[82–84] the exponential formula (1),[82,83] and the polynomial forms (3) and (4) [84] are used, i.e.,

$$f(n) = C_0 + C_1 e^{-(n-1)} + C_2 e^{-(n-1)^2}, \quad lim_{n\to\infty} f(n) = C_0, \tag{1}$$

$$g(n) = C_0 + C_1 e^{-C_2 n}, \quad lim_{n\to\infty} g(n) = C_0, \tag{2}$$

$$h(n) = C_0 + \frac{C_1}{(x+1/2)^4}, \quad lim_{n\to\infty} h(n) = C_0, \tag{3}$$

$$z(n) = C_0 + \frac{C_1}{n^3}, \quad lim_{n\to\infty} z(n) = C_0, \tag{4}$$

where C_i are the extrapolation parameters fitted to our dataset, x is the zeta size of the basis set, and $C_2 > 0$ in $g(n)$.

III. RESULTS AND DISCUSSION

A. Bonding analysis

The chemical bonds of Mo_2 determine and affect its chemical properties and the reactivity of its dimolybdenum complexes. The ground atomic term of each Mo atom in the Mo_2 molecule is ^{7}S, which gives rise to Λ-S states with $\Lambda = 0$ and alternating $\hat{i}$ symmetry, i.e.,

$$^7S \otimes {}^7S = {}^1\Sigma_g^+ \otimes {}^3\Sigma_u^+ \otimes {}^5\Sigma_g^+ \otimes {}^7\Sigma_u^+ \otimes {}^9\Sigma_g^+ \otimes {}^{11}\Sigma_u^+ \otimes {}^{13}\Sigma_g^+.$$

It is interesting that all seven states, apart from $^{13}\Sigma_g^+$, have multireference character (see Table II). The main configuration of the ground state contributes 80% to the total wavefunction, while for the septet state, the main configuration contributes only 25%, showing that an HF picture is not adequate.

TABLE II. Coefficients and main configurations (only valence electrons are included) of the ground and low-lying Mo_2 states at the CASSCF(MRCISD)/aug-cc-pVQZ-PP level of theory.

State	Coefficient	Configuration
$^1\Sigma_g^+$	0.803(0.771)	$\lvert\pi_u^4\sigma_g^2\delta_g^4\sigma_g^2\rangle$
$^3\Sigma_u^+$	0.483(0.475)	$\lvert\pi_u^4\sigma_g^2\sigma_g^2\delta_g^3\delta_u^1\rangle$
$^5\Sigma_g^+$	0.553(0.557)	$\lvert\pi_u^4\sigma_g^2\sigma_g^2\delta_g^2\delta_u^2\rangle$
$^7\Sigma_u^+$	0.246(0.262)	$\lvert\sigma_g^2\pi_u^4\sigma_g^1\delta_g^2\delta_u^2\sigma_u^1\rangle$
$^9\Sigma_g^+$	0.284(0.296)	$\lvert\sigma_g^2\pi_u^3\sigma_g^1\delta_g^2\delta_u^2\sigma_u^1\pi_g^1\rangle$
$^{11}\Sigma_u^+$	0.546(0.578)	$\lvert\sigma_g^2\pi_u^2\sigma_g^1\delta_g^2\delta_u^2\sigma_u^1\pi_g^2\rangle$
$^{13}\Sigma_g^+$	1.000(0.962)	$\lvert\sigma_g^1\pi_u^2\sigma_g^1\delta_g^2\delta_u^2\sigma_u^1\pi_g^2\sigma_u^1\rangle$

1. Ground $X^1\Sigma_g^+$ state

The ground state of Mo_2 has a sextuple bond: two σ_g, two π_u, and two δ_g bonds. The molecular orbital plots and their CASSCF energies of the bonding molecular orbitals are depicted in Fig. 1. Furthermore, the bonding (two σ_g, two π_u, and two δ_g) and the antibonding (two δ_u, two π_g and two σ_u) orbitals are depicted in Fig. 1S of the supplementary material. In order of increasing energy, the π_u bonds are the strongest ones, following by the $1\sigma_g$ bond, then about 3 eV higher in energy are the δ_g and $2\sigma_g$ bonds. The π_u bonds are formed between two d_{xz} and two d_{yz} atomic orbitals, the δ_g bonds are formed between two d_{x2-y2} and two d_{xy} orbitals, and the σ_g bonds are formed between 5s and 5s and $4d_{z2}$–$4d_{z2}$ orbitals. The σ bond resulting from the $4d_{z2}$–$4d_{z2}$ atomic orbitals is stronger than the σ bond resulting from 5s-5s. Note that the last bond is energetically the weakest one. Moreover, it should be mentioned that there is a small 4d5p hybridization in π and σ bonds. The bonding molecular orbitals are composed of the following atomic orbitals with the listed coefficients: $\phi_{\pi_u} = (0.62d_{xz} + 0.11p_x) + (0.62d_{xz} + 0.11p_x)$ and $\phi_{\pi_u} = (0.62d_{yz} + 0.11p_y) + (0.62d_{yz} + 0.11p_y)$; $\phi_{1\sigma_g} = (0.61d_{z2} + 0.11p_z) + (0.61d_{z2} + 0.11p_z)$; $\phi_{\delta_g} = (0.66d_{x2-y2}) + (0.66d_{x2-y2})$ and $\phi_{\delta_g} = (0.66d_{xy}) + (0.66d_{xy})$; $\phi_{2\sigma_g} = (0.57s + 0.12p_z) + (0.57s + 0.12p_z)$.

The main electronic configuration of the ground state is $|\pi_u^4\sigma_g^2\delta_g^4\sigma_g^2\rangle$. We can categorize the molecular bonding orbitals in two groups. These groups are referred to here as "shells." Each shell contains three bonds, one with $\Lambda = 0$ and two degenerate $\Lambda \neq 0$. The two shells differ in energy by about 3 eV, and in both cases, the orbitals with higher angular momentum $\Lambda = 1, 2$ have lower energy than those with $\Lambda = 0$. Thus, the ground state main electronic configuration is $|\pi_u^4\sigma_g^2\delta_g^4\sigma_g^2\rangle$. The calculated order of the inner π_u-σ_g orbitals contradicts the results obtained in previous quantum-Monte Carlo studies.[66] Their lower energy orbital is found to be σ_g. Here, the shell-like structure of the dimer is the key for understanding its chemical properties, while it can be explained by considering the effects of the Coulombic repulsions and Pauli correlations of the electrons. It is found that the π_u molecular orbitals are lower in energy than σ_g in the first shell and δ_g is lower in energy than σ_g in the second shell meaning that the overlapping is weaker in σ bonds than in π and δ in each shell. Apart from the electromagnetic interaction, the electrons are correlated through the Pauli principle. This fermionic effect tends to keep electrons with the same energy and spin at greater distances. Consequently, the two σ orbitals cannot have close energy values and the system favors a state where they are allocated into two different shells. The interplay of the Pauli correlations and repulsive/attractive forces, which creates shell-like structures in the quantum ground states, is present in many N-body saturated fermionic systems, such as the ground state shell structure of the atomic nuclei.

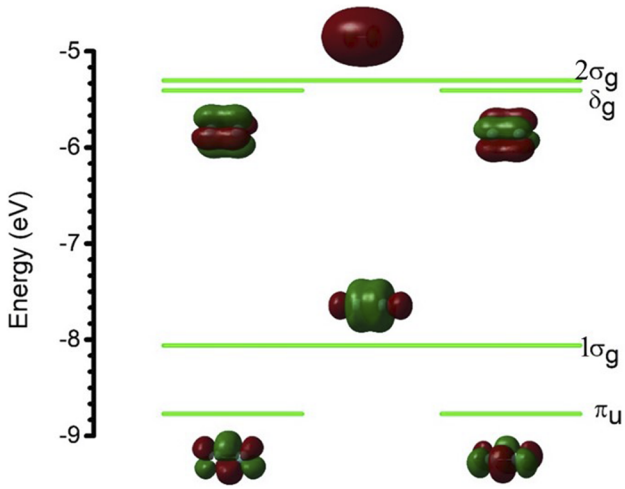

FIG. 1. Molecular orbital diagram of the $X^1\Sigma_g^+$ state of Mo_2 at CASSCF/aug-cc-pVQZ-PP. $1\sigma_g$ corresponds to the $4d_z^2$–$4d_z^2$ bond and $2\sigma_g$ corresponds to the 5s–5s bond.

2. Low-lying excited states

As mentioned above, all calculated excited states (except for the 2S + 1 = 13) have a highly multireference character (see Table II). Their CASSCF molecular orbital diagram is depicted in Fig. 2. Each excited state has one less bond than the previous state, i.e., the triplet state has five bonds, the quintet four bonds, the septet three bonds, the nonet two bonds, and the undecet one bond, while the $^{13}\Sigma_g^+$ state is a weakly bound dimer due to weak interactions between $5s^1\cdots5p_z{}^0$ from one Mo atom to the other one, see below.

The energy and symmetry of the molecular orbitals of the excited states can be explained by the same reasoning that was used for the ground state. As the spin multiplicity increases, the electrons are promoted to higher energy orbitals with different $\hat{i}$ symmetries. The order of the "breaking" of bonds follows the energy ordering of the shells. As the total spin increases, the three bonds of the outer shell are broken first, and then, the three bonds of the inner shell follow suit. However, it is interesting that while in the singlet, triplet, and quintet states, the $1\sigma_g{}^2$ molecular orbital is a $4d_{z2}{}^{\uparrow}$–$4d_{z2}{}^{\downarrow}$ bond; in the remaining states with 2S + 1 = 7, 9, and 11, the $1\sigma_g{}^2$ molecular orbital is a $5s^{\uparrow}$–$5s^{\downarrow}$ bond. This happens because the $4d_{z2}$ orbitals form a shorter bond than the 5s orbitals.[34,35]

The fact that orbital energies converge as one moves to higher multiplicity states can be explained in two ways. (A) The system favors states with excited $\Lambda \neq 0$ electrons to minimize the Pauli correlations of the electrons. In that way, the electrons with parallel spins are found at greater intermediate distances. Therefore, the energy order of the orbitals changes from the singlet to the triplet state and then to the quintet state. In the septet state, the $1\sigma_g$ and $2\sigma_g$ orbitals tend to have greater energy differences and consequently are further apart in order to minimize their Pauli correlations. Then, the system reduces the σ_{1g} orbital's energy and it is more stabilized than the π_u at higher spin multiplicities and it has a different character; it is a 5s–5s bond. The exchange of the inner shell orbitals is observed in the shape of the PEC of the $^7\Sigma_u^+$ state. It causes a non-avoided crossing at r = 2.2 Å due to the change of the orbital ordering along the PEC. For r < 2.2 Å, the π_u bonds are more stable than $\sigma_g(4d_{z2}$–$4d_{z2})$. However, for r > 2.2 Å, the $\sigma_g(5s$–$5s)$ bond becomes energetically stronger than π_u. An additional observation from the diagram in Fig. 2 is the gradual disappearance of the shell structure of the excited states. As the spin multiplicity increases and a greater number of electrons are promoted to higher energy "virtual" orbitals, the total energy of the system increases. The two shells then

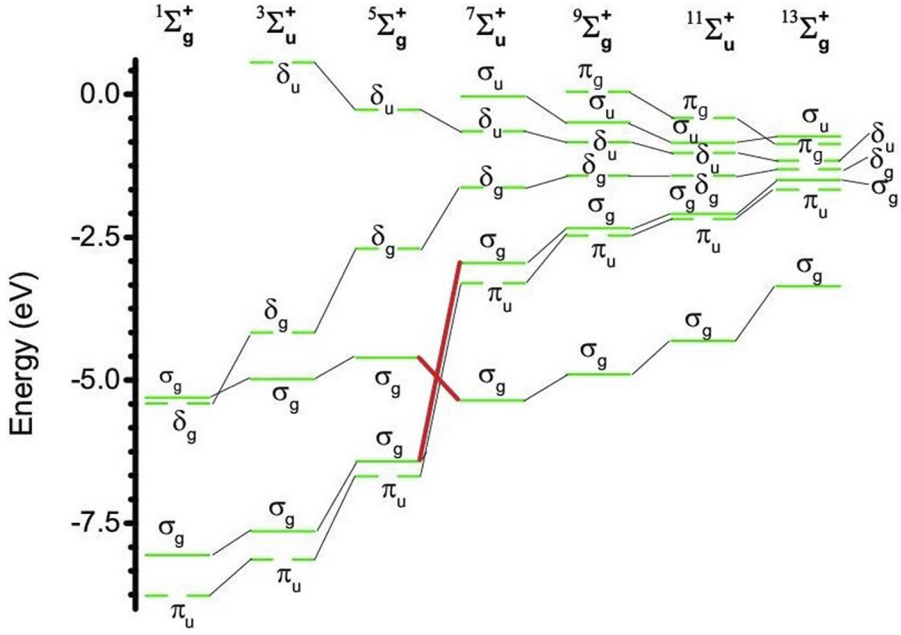

FIG. 2. CASSCF/aug-cc-pVQZ-PP molecular orbital diagram of the Σ^+ states of Mo_2 at the potential energy minimum of each state.

collapse in intermediate energies and the shell structure is gradually lost, as the 2S + 1 is increased. (B) The bond length is increasing as the multiplicity increases. Thus, due to decreased orbital overlap at longer bond lengths, one would expect the corresponding bonding and antibonding pairs of orbitals to get closer in energy, eventually merging at the energy of the orbitals in the isolated atoms at long distances. This also explains why the separation between the δ_g and δ_u orbitals converges first, as these overlap the least. This is followed by a convergence of the bonding π_u and antibonding π_g orbitals at longer distances. The σ_g/σ_u orbitals deriving from the 5s are the slowest to converge because these atomic orbitals continue to overlap even at relatively long distances. This is a major contributor to the reversal in energy ordering between the $1\sigma_g$ and $2\sigma_g$ orbitals, which occurs in the higher multiplicity states.

Experimentally, two excited states have been observed, which are matching nicely with our calculated states. Kraus *et al.*[46] via matrix isolation fluorescence studies observed phosphorescence from a state lying at approximately T_0 = 7977.6 cm^{-1} above the ground state that matches fairly nicely with the $^3\Sigma_u^+$ state calculated to lie at T_e = 0.916 eV = 7391 cm^{-1} (Table III). The experimentally estimated vibrational frequency is 393.7 cm^{-1} in good agreement with our calculated value of 351.7 cm^{-1}. Moreover, another excited state lying at T_0 = 13 747 cm^{-1} was found to phosphoresce to the ground state.[43,47] This is lying in the right range to correspond to the $^5\Sigma_g^+$ state that is calculated to lie at 1.776 eV (14 324 cm^{-1}).

Finally, the $^{13}\Sigma_g^+$ state has a different type of bond. The molecule in this state is a weakly bound dimer having two weak σ bond interactions between $5s^1\cdots5p_z^0$ from one Mo atom to the other one. The Mulliken charges on each Mo atom are $5s^{0.9}5p_z^{0.1}$, showing that there is a small charge transfer from one Mo atom to the second one through one weak σ bond and backward through the second σ bond interaction. The corresponding molecular orbitals are: $\sigma^1 = |[0.7(5s)$

TABLE III. Bond lengths r_e (Å), dissociation energies D_e and D_0 (eV), harmonic frequencies and anharmonic corrections ω_e, $\omega_e\chi_e$ (cm^{-1}), rotational constants B_e and D_J (cm^{-1}), energy differences T_e (eV), and energy separation $\Delta_{S,S-1}$ (cm^{-1}) of the seven calculated states of Mo_2 at the MRCISD+Q(MRCISD)/aug-cc-pVQZ-PP level of theory.

State	r_e	D_e	D_0	ω_e	$\omega_e\chi_e$	B_e	$D_J(\times10^{-8})$	T_e	$\Delta_{S,S-1}$
$X^1\Sigma_g^+$	1.9561	3.515(3.172)	3.492	370.5	1.21	0.088	1.999	0	0
$^3\Sigma_u^+$	2.0727	2.600(2.227)	2.534	351.7	1.48	0.079	1.567	0.916	7391
$^5\Sigma_g^+$	2.1911	1.741(1.372)	1.675	273.5	1.33	0.070	1.857	1.776	6933
$^7\Sigma_u^+$	2.6579	0.978(0.713)	0.912	117.0	0.43	0.048	3.185	2.539	6153
$^9\Sigma_g^+$	2.9127	0.681(0.480)	0.616	127.9	0.74	0.040	1.538	2.835	2389
$^{11}\Sigma_u^+$	3.1009	0.380(0.242)	0.314	106.9	0.93	0.035	1.513	3.136	2430
$^{13}\Sigma_g^+$	3.6307	0.098(0.066)	0.032	45.5	0.66	0.026	3.238	3.419	2279

+ 0.1(5p$_z$)]$_{Mo}$ ± [0.7(5s) − 0.1(5p$_z$)]$_{Mo'}$⟩. Moreover, we could say that this state resemblance the Be_2 bond where one beryllium atom donates an electron pair to the second one, and vice versa,[85] but in the case of the $^{13}\Sigma_g^+$ state of Mo_2, one Mo atom donates one 5s electron instead of the electron pair of Be. The total bond energy of the $^{13}\Sigma_g^+$ state is 971 cm^{-1}, i.e., 486 cm^{-1} for each interaction, see below.

B. Spectroscopic parameters and potential energy curves

The MRCISD+Q potential energy curves (PECs) of the seven calculated states of Mo_2 are depicted in Fig. 3. Their bond distances, dissociation energies, spectroscopic parameters, and relative energy differences are given in Table III. Given a large number of valence electrons, the addition of +Q correction is significant. Thus, the MRCISD+Q dissociation energies are larger than the MRCISD by 10%–35%. The largest increase is observed for the states with 2S + 1 = 9, 11, and 13 (see Table III and Table 2S of the supplementary material).

1. $X^1\Sigma_g^+$ state: Comparison of methodologies and CBS limits

Four different types of basis sets have been used to study the quasi-relativistic Mo_2 (see Table IV). Two types of relativistic pseudopotentials, where the scalar relativistic effects are implicitly parameterized inside them, are used. One method treats the correlation of the (5s4d)[6] electrons while the other additionally includes the correlation of the $4s^24p^6$ electrons. The inclusion of $4s^24p^6$ in the correlated space leads to a shrinkage of the calculated bond length of 0.009 Å, but the most important effect of this inclusion is the significant increase of the dissociation energy by 0.74 eV, which is an increase of 21% of the dissociation energy. Thus, the $4s^24p^6$ electrons can be regarded as semi-valence electrons.

In addition to the use of basis sets with pseudopotentials, we applied the Douglas–Kroll decoupling method up to the ninth order to describe the scalar effects (momentum–velocity and Darwin corrections) including or omitting the correlation of the semi-valence $4s^24p^6$ electrons (DK9 and wC-DK9 columns in Table IV). It should be noted that comparing DK2 and DK9, only a small difference of 0.002 Å is found for the Mo–Mo bond distance at the RCCSD[T] level of theory. Comparing C-RCCSD[T]-DK9/aug-cc-pwCVTZ-DK and C-RCCSD[T]/aug-cc-pwCVTZ-PP, we observe that the Douglas–Kroll approach presents similar data regarding bond length, while the dissociation energy is larger by about 0.2 eV than the value of the PP approach. However, the increase of the basis set from triple to quadruple results in a larger D_e by 0.04 eV than the DK9 approach. Thus, the C-RCCSD[T]/aug-cc-pwCVQZ-PP level can be considered as a better approach than C-RCCSD[T]-DK9/aug-cc-pwCVTZ-DK.

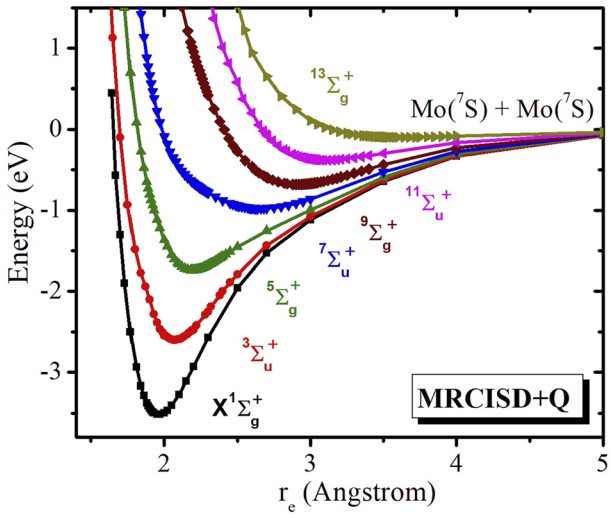

FIG. 3. PECs of the seven calculated states of Mo_2 correlating to the Mo(^{7}S) + Mo(^{7}S) separated atom limit at the MRCISD+Q/aug-cc-pVQZ-PP level of theory.

TABLE IV. Bond lengths r_e (Å), dissociation energies D_e and D_0 (eV), and harmonic frequencies and anharmonic corrections ω_e, $\omega_e\chi_e$ (cm^{-1}) of the $^1\Sigma_g^+$ state of Mo_2 at RCCSD[T] level of theory using different types of basis sets. Experimentally derived values are also included.

	DK9[a]	wC-DK9[b]	wC-PP[c]	PP[d]	wC-PP[e]	Expt.
r_e	1.9534	1.9428	1.9434	1.9464	1.9372	1.929,[f] 1.938(9)[g]
D_e	3.550	4.306	4.122	3.603	4.347	4.476(10)[h]
D_0	3.484	4.277	4.056	3.537	4.282	
ω_e	462.1	474.5	477.7	470.7	488.5	477.1[f]
$\omega_e\chi_e$	1.87	1.60	1.72	1.91	1.70	1.51[f]

[a]RCCSD[T]-DK9/aug-cc-pVTZ-DK.
[b]C-RCCSD[T]-DK9/aug-cc-pwCVTZ-DK.
[c]C-RCCSD[T]/aug-cc-pwCVTZ-PP.
[d]RCCSD[T]/aug-cc-pVQZ-PP.
[e]C-RCCSD[T]/aug-cc-pwCVQZ-PP.
[f]Reference 42.
[g]Reference 44.
[h]Reference 45.

Comparing the calculated values at the C-RCCSD[T]/aug-cc-pwCVQZ-PP level of theory with the experimental ones, we observe that the calculated bond length of 1.9372 Å is in excellent agreement with the experimental values of 1.929[42] and 1.938(9)[44] Å. Moreover, the calculated dissociation energy D_e is 4.347 eV is in very good agreement with the experimental D_0 of 4.476(10) eV,[45] i.e., there is a small underestimation of 0.13 eV. Below, benchmark coupled cluster calculations are carried out using a series of basis sets, aug-cc-pwCVnZ-PP, n = 2–5 to calculate the CBS limit for the calculated values.

2. Benchmark calculations: CBS limit

Four extrapolation schemes [Eqs. (1)–(4)] are used to calculate the C-RCCSD[T] CBS limits of the r_e, D_e, D_0, ω_e, and $\omega_e\chi_e$ values (see Table V). The plots of the extrapolation formulas are depicted in Fig. 4. All four extrapolation schemes predict almost the same CBS values in excellent agreement with the experimental values. The CBS limits of r_e differ slightly up to 0.001 Å and the D_e values up to 0.08 eV. We consider the exponential and mixed Gaussian/exponential formula as our best values. The extrapolations obtained by these two methods were averaged to obtain our best values. Thus, our final values are r_e = 1.9324 Å and D_e (D_0) = 4.502 ± 0.007(4.471 ± 0.009) eV, which are in excellent agreement

TABLE V. Bond lengths r_e (Å), dissociation energies D_e and D_0 (eV), and harmonic frequencies and anharmonic corrections ω_e, $\omega_e\chi_e$ (cm^{-1}) of the $X^1\Sigma_g^+$ and $^{13}\Sigma_g^+$ state of Mo_2 at C-RCCSD[T]/aug-cc-pWCV*n*Z-pp, *n* = D(2), T(3), Q(4), and 5 level of theory. Experimental values are also included.

x	r_e	D_e	D_0	ω_e	$\omega_e\chi_e$
			$X^1\Sigma_g^+$		
2(D)	1.9677	3.556	3.490	458.7	1.83
3(T)	1.9434	4.122	4.056	477.7	1.72
4(Q)	1.9372	4.347	4.282	488.5	1.70
5	1.9336	4.448	4.382	490.5	1.68
Expt.	1.929,[a] 1.938(9)[b]		4.476(10)[c]	477.1[a]	1.51[a]
CBS(f)[d]	1.9324	4.494	4.463	493.3	1.68
CBS(g)[d]	1.9327	4.511	4.480	494.3	1.68
CBS(h)[d]	1.9336	4.430	4.399	490.1	1.68
CBS(z)[d]	1.9324	4.460	4.429	491.2	1.67
			$^{13}\Sigma_g^+$		
4(Q)	3.527	0.120	0.117	50.9	0.8

[a]Reference 42.
[b]Reference 44.
[c]Reference 45.
[d]Equations (1)–(4).

with the experimental values of r_e = 1.929[42] and 1.938(9)[44] Å and D_0 = 4.476(10)[45] eV.

3. Excited states of Mo_2

The bond distances, dissociation energies, spectroscopic parameters, and relative energy differences of the calculated seven states of Mo_2, at MRCISD+Q/aug-cc-pVQZ-PP, are given in Table III, and they are plotted with respect to the spin multiplicity in Fig. 5. As the spin multiplicity increases, the bond length increases, while the bond energy, vibrational, and anharmonicity parameters decrease as expected. An interesting characteristic of the plots in Fig. 5 is a discontinuity at the parameters of the septet state. This probably occurs because, as it is mentioned in Sec. III A 2, the σ_g molecular orbital for the states with 2S + 1 = 7–11 has a different character, i.e., it is a 5s–5s bond, and it is the strongest molecular orbital. On the contrary, for the states with 2S + 1 = 1–5, the π_u orbitals are the lowest energy molecular orbitals, followed by a σ_g orbital that is a d_{z2}–d_{z2} bond. Note that, for the state with 2S + 1 = 13, the lowest molecular orbital is a singly occupied σ_g orbital, $5s\cdots5p_z$. Thus, regarding the r_e values, for the states with 2S + 1 = 1–5, the increase of r_e is linear, the three r_e are lying in the same straight line, then there is a gap, and the r_e of the states with 2S + 1 = 7–11 is lying in another straight line. Then, there is a second gap for the state with 2S + 1 = 13. Similarly, regarding the D_e values, they are lying in a straight line for the states with 2S + 1 = 1–5, and the D_e values of the states with 2S + 1 = 7–13 are lying in another straight line (see Fig. 5).

We observe that the energy separation $\Delta_{S,S-1}$ of the seven calculated states of Mo_2 remains the same in groups. Specifically, the energy difference between singlet, triplet, and quintet is about 7000 cm^{-1}, the difference between quintet and septet states is smaller, i.e., 6200 cm^{-1}, and the difference between septet, nonet, and 2S + 1 = 13 is about 2300 cm^{-1}. The reduction of the energy difference between quintet and septet is attributed to the fact that the σ bond changes character from quintet to septet and it becomes the most stable bond in septet, while in the singlet, triple, and quintet states, the π bonds are the most stable ones (see Fig. 2). Note that, for the septet state in 2.31 Å, which is the bond distance where it

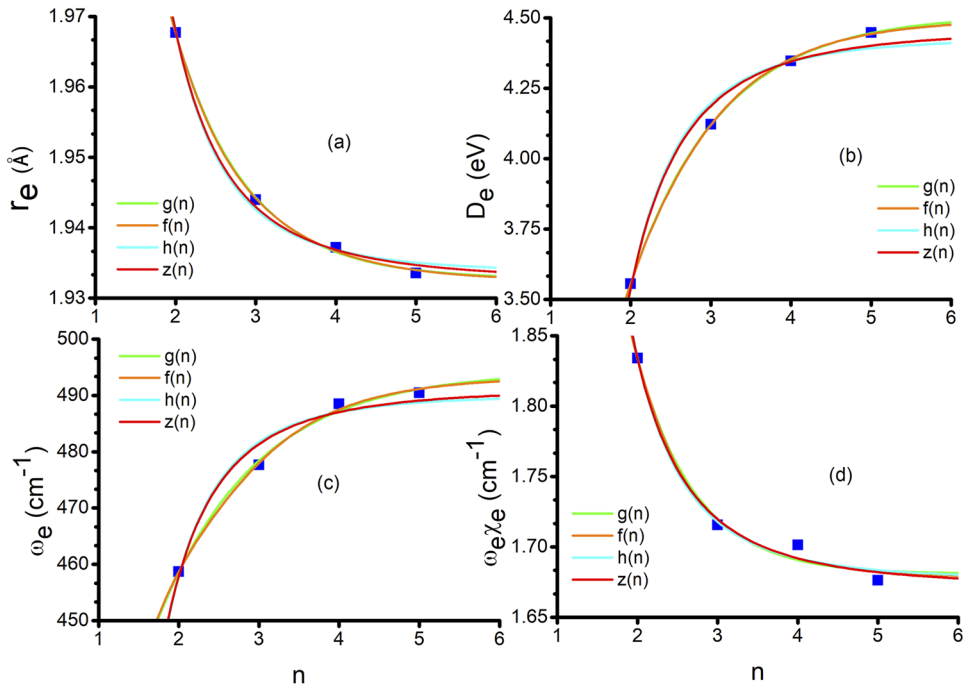

FIG. 4. Extrapolation plots of C-RCCSD[T]: (a) bond distances r_e, (b) dissociation energies D_e, (c) harmonic frequencies ω_e, and (d) $\omega_e\chi_e$ with respect to the basis set size, aug-cc-pwCV*n*Z-PP, *n* = D(2), T(3), Q(4), 5 of the $X^1\Sigma_g^+$ state.

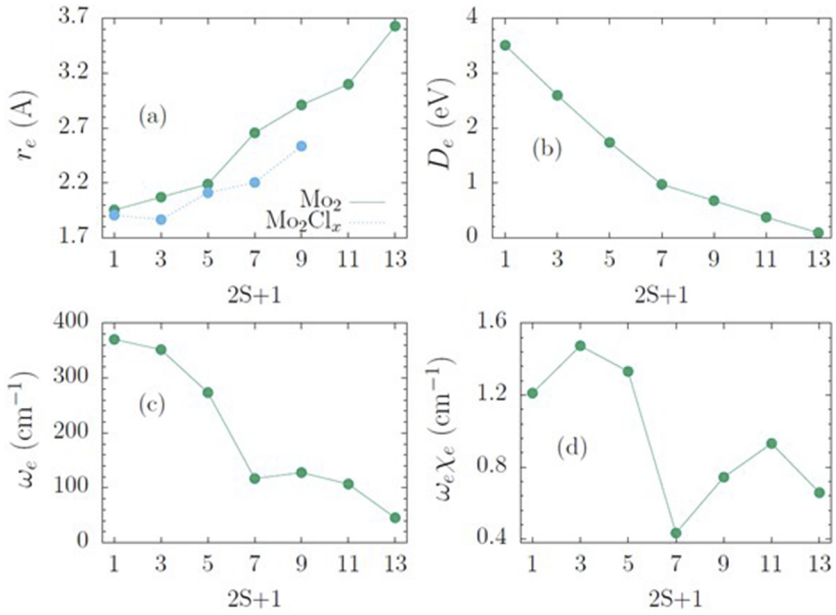

FIG. 5. Plots of r_e (a), D_e (b), ω_e (c), and $\omega_e\chi_e$ (d) with respect to the spin multiplicity at MRCSID+Q/aug-cc-pVQZ-PP. The cyan curve corresponds to the *r*(Mo–Mo) bond length for the Mo_2Cl_x x = 0,2–8 complexes at the TPSSH/aug-cc-pVTZ-PP level of theory.

would be expected to be the minimum if there was not a change in the type of the σ bond, the energy difference between quintet and septet is about 7500 cm^{-1}, close to the energy difference of the three lowest in spin states.

In the $^{13}\Sigma_g^+$ state, Mo_2 is a weakly dimer, where two $5s^1\cdots5p_z^0$ bonds are formed at 3.527 Å. Its PEC at C-RCCSD[T]/aug-cc-pwCVQZ-PP level of theory is plotted in Fig. 6. The binding energy is D_e = 0.120 eV (971 cm^{-1}), i.e., each $5s\cdots5p_z$ single bond interaction corresponds to 0.060 eV (486 cm^{-1}). This state resembles the Mn_2 molecule, which is a van der Waals type dimer in its six lowest energy states.[86] In Mn_2, the Mn (^{6}S) atoms interact via van der Waals bond and it is hardly influenced by the total spin. As a result, the six Σ states, singlet to undecet states ($X^1\Sigma_g^+$, $^3\Sigma_u^+$, $^5\Sigma_g^+$, $^7\Sigma_u^+$, $^9\Sigma_g^+$, and $^{11}\Sigma_u^+$), are in essence degenerate packed within an energy interval of about 70 cm^{-1}. Their ordering follows the spin multiplicity, the ground state being a singlet, $X^1\Sigma_g^+$, with binding energy De (D_0) about 600(550) cm^{-1} at r_e = 3.60 Å. Here, the $^{13}\Sigma_g^+$ state of Mo_2 has twice this bond energy at the same bond distance comparing to the $^{1,3,5,7,9,11}\Sigma^+$ states of Mn_2. This shows that, in Mo_2, the interaction due to two $5s\cdots5p_z$ interaction is much stronger than the interaction of Mn_2.

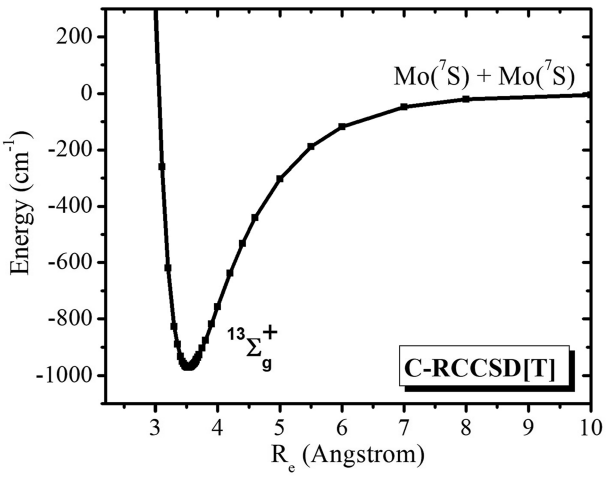

FIG. 6. PEC of the $^{13}\Sigma_g^+$ state of Mo_2 at the C-RCCSD[T]/aug-cc-pwCVQZ-PP level of theory.

4. Mo_2Cl_x complexes, x = 2–8

The six calculated excited states of Mo_2 with 2S + 1 = 3–13 can be related to specific dimolybdenum complexes (Fig. 7). Thus, Mo_2Cl_x complexes having Mo–Mo multiple bonds whose multiplicity decreases as the number x of the attached Cl increases are investigated to add physical insight into the nature of the sextuple bond and its dissociation energy. Only singlet states of the Mo_2Cl_x complexes are calculated. The Cartesian coordinates and their frequencies are given in the supplementary material (Tables 3S and 4S). The lowest in energy minima of the Mo_2Cl_x complexes have been calculated. When more than one structure has been calculated, the relative energies are given. In the case of Mo_2Cl_4, Mo_2Cl_8, and Mo_2Cl_{10}, two, four, and one additional structures have been calculated, which are minima, transition states, or saddle points (see Fig. 7). It is of interest that, in the case of Mo_2Cl_4, the global minimum (a) is not a planar structure; the planar structure is a saddle point with two imaginary frequencies (see Table 4S of the supplementary material). It should be noted that there is not any spin contamination for all these species. We may understand the structure of the Mo_2Cl_x complexes, n = 2, 4, 6, and 8, as the result of covalent bond formation between the chlorines and the excited

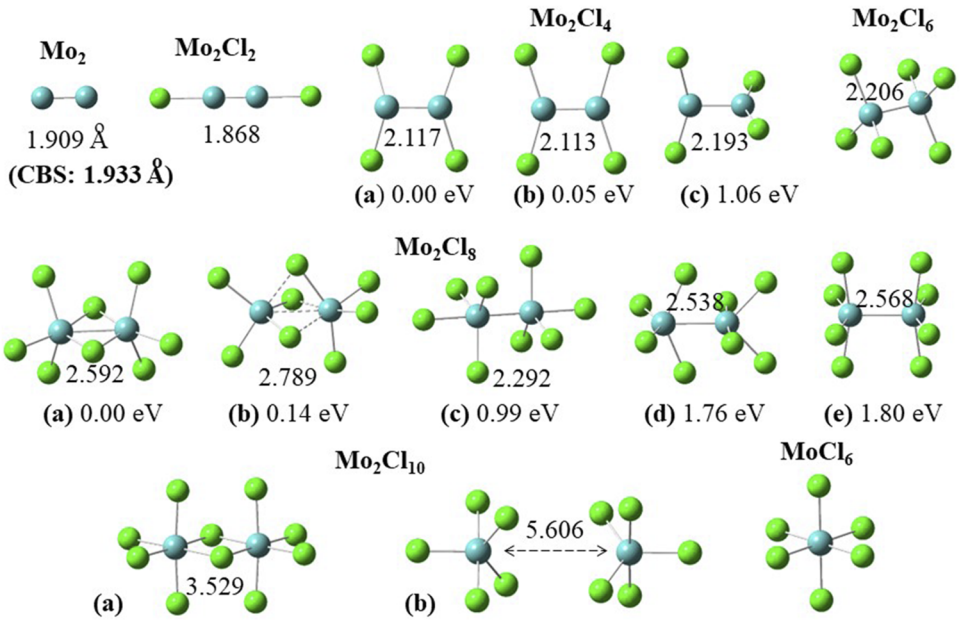

FIG. 7. Calculated Mo_2Cl_x and $MoCl_6$ complexes at TPSSh/aug-cc-pVTZ $(\text{-PP})_{Mo}$ level of theory. Mo–Mo distances, relative energies at TPSSh/aug-cc-pVTZ$(\text{-PP})_{Mo}$, and the CBS limit at C-RCCSD[T]/aug-cc-pwC*n*Z-PP are given.

states of the Mo_2 metallic center with 2S + 1 = 3, 5, 7, and 9, respectively. Thus, each pair of chlorine atoms is bonded with a state of a higher spin multiplicity since a bond from the original ground state dimer is broken. Given this perspective, we did not conduct a comprehensive study of all possible structures of Mo_2Cl_x, such as $MoClClMoCl_{x-2}$ structures or structures having a multiplicity of spin $2S + 1 \neq 1$. In other words, we looked at the first step of chlorine addition reactions, which causes a stepwise reduction of the multiplicity of the Mo–Mo bond.

In Fig. 5(a), the TPSSH Mo–Mo distance in Mo_2Cl_x complexes is plotted with respect to $n + 1$, which corresponds to 2S + 1 in the Mo_2 molecule. The r_e bond length of the X state of Mo_2 at the TPSSH/aug-cc-pVTZ-PP is shorter by 0.05 Å than at the corresponding value MRCISD+Q/aug-cc-pVQZ-PP level, but here the general trend is what is examined. It is interesting that the Mo–Mo distance in the Mo_2Cl_2 complex is shorter than in Mo_2 at the same level of theory, showing that the Mo–Cl bonding makes the Mo–Mo bonds stronger in Mo_2Cl_2. However, as the next Mo–Mo covalent bond is broken due to the formation of new Mo–Cl bonds, the Mo–Mo bond length is increased. Thus, as x is increased, the Mo–Mo bond length is also increased but less than in the case of the corresponding excited states of Mo_2. This may be reasoned by considering the allocation of electronic density from the dative bonds of the Cl ligands to the metallic dimer center. For $n = 10$, the formation of five equivalent covalent bonds with Cl, while the Mo–Mo distance is similar to this of the $^{13}\Sigma_g^+$ state of Mo_2, is not possible due to the structural constraints resulting from the size in Cl for this Mo–Mo distance. In this case, the two Mo atoms are kept apart, see Fig. 6 (structure b). In the global minimum of Mo_2Cl_{10} (structure a), each Mo forms covalent bonds with four Cl atoms, with the remaining two Cl atoms forming two bridges with both Mo (see Fig. 6). This molecule[87] forms a dark volatile solid that is used to prepare other molybdenum compounds. There are two possible interpretations of the bonding. It could be regarded that each Mo forms five covalent bonds with five Cl atoms, while an additional weak σ interaction is formed between the two Mo atoms, and dative interactions $5p^0 \leftarrow 3p^2$ between Mo and the Cl that form a covalent bond with the other Mo atom. In the second interpretation of the bonding, it could be regarded that one Mo atom forms six covalent bonds with six Cl atoms (see Fig. 6), while the second Mo atom is in a ^5D state ($5s^24d^4$) forming dative bonds with the Cl atoms of the bridge, i.e., $4d^0 \leftarrow 3p^2$ and $5p^0 \leftarrow 3p^2$. Note that the distance between the two Mo atoms is the same as the distance of the $^{13}\Sigma_g^+$ state of Mo_2. It should be noted that the molecular orbitals are mixed (see the supplementary material), and it is not possible to decide which one is the case of the bonding in Mo_2Cl_{10}. However, the first interpretation seems to be the most favorable energetically since no excited states of Mo are involved. Moreover, the binding energy of each Mo–Cl bond is calculated here at 3.2 eV in $MoCl_6$, while in Mo_2Cl_{10} is calculated at 3.5 eV at TPSSH/aug-cc-pVTZ$(\text{-PP})_{Mo}$ showing that there should be an interaction between the two Mo atoms. However, in both interpretations even though there are additional interactions, each Mo has six bonds in agreement with Chen *et al.*[62]

For the Mo_2Cl_2 molecule, the energy ordering of its molecular orbitals is provided in Fig. 8. These molecular orbitals are constructed from the valence 3s3p, and 4d5s atomic orbitals of Cl and Mo, respectively. The original six σ, π, and δ orbitals of the free Mo_2 ($^3\Sigma_u^+$) dimer are mixed with the atomic orbitals of the chlorines (^2P) and new linear combinations are constructed. Nevertheless, the basic shell structure is maintained. We consider that the $1\delta_g$, $3\sigma_g$, $2\pi_u$, and $1\sigma_g$ complex orbitals are participating mostly in the Mo–Mo bond and, thus, are comprised mostly from the free dimer's orbitals. The $1\delta_g$ complex orbital is essentially the same as the free orbital, the $3\sigma_g$ and $1\sigma_g$ are constructed from the free corresponding orbitals and the $3p_z$ and 3s orbitals of chlorines, respectively, and the $2\pi_u$ orbitals are a combination of the corresponding free and

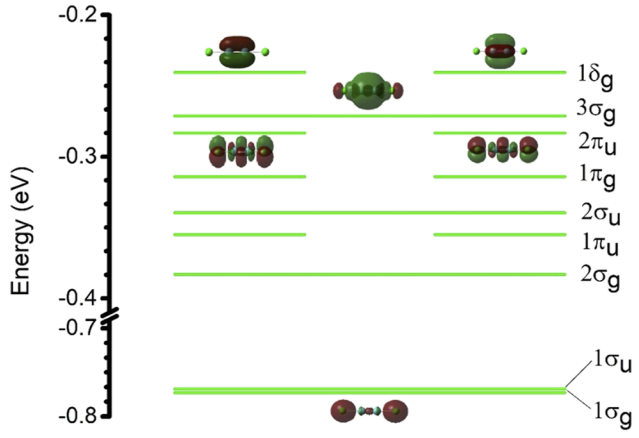

FIG. 8. Molecular orbital diagram for the ground state of Mo_2Cl_2. The orbital energies are calculated at the TPSSH/aug-cc-pVTZ-PP level of theory. The $1\delta_g$, $3\sigma_g$, $2\pi_u$, and $1\sigma_g$ orbitals that participate in the Mo–Mo bond are plotted.

$3p_x$ and $3p_y$ of chlorines. The orbital "shell-like" structure of the complex is reminiscent of the $^3\Sigma_u^+$ Mo_2 state, with five bonds created by the aforementioned orbitals. The LUMO complex orbital has a δ_u character just as the HOMO orbital of the dimer, while the inner σ orbital has a lower energy than the π orbitals in the complex. This can be reasoned according to the stabilization due to the electronic density given by the 3s Cl orbitals to the metallic center. Interestingly, the almost degenerate $1\sigma_u$ orbital that mostly participates in the Mo–Cl bonds is constructed by the 3s Cl and $5p_z$ Mo atomic orbitals. This is additional evidence of the 5p orbital participation in the bonding of the Mo_2 dimer and complexes.

In addition, in accordance with the chemical bonding in the Mo_2Cl_2 complex, DFT calculations on quintuply bonded $[Mo_2\{\mu\text{-}\eta^2\text{ –RC(N-2,6-}i\text{Pr}_2\text{C}_6\text{H}_3)_2\}_2]$ (R = H, Ph) complex[69] show similar chemical bonding. In this complex, its metallic dimer main configuration is $|\pi^4\sigma^2\delta^4\rangle$, which agrees with the orbital ordering of Fig. 2. Finally, for the triple bonded $K_3[Mo_2(HPO_4)_4]$ complex salt,[88] its main configuration is determined spectroscopically to be $|\sigma^2\pi^4\delta^1\rangle$. The inversion of the σ and π orbitals resembles the reverse ordering of the septet state.

IV. CONCLUSIONS AND FINAL REMARKS

In this study, we perform very accurate calculations via multireference configuration interaction and coupled cluster methodologies on the dimolybdenum molecule, i.e., MRCISD, MRCISD+Q, and C-RCCSD[T], in conjunction with aug-cc-pCV*n*Z-PP, aug-cc-pVTZ-DK, and aug-cc-pwCV*n*Z-PP, *n* = D, T, Q, and 5. The bonding, the dissociation energies, and the spectroscopic parameters of the seven states that correlate with the ground state products are calculated. As far as we know, the excited states of Mo_2 have not been calculated before. The calculated values for the ground $X^1\Sigma_g^+$ and the $^{13}\Sigma_g^+$ states of Mo_2 have been extrapolated to the CBS limits. The sextuple bond breaking of Mo_2, as the spin multiplicity is increased, and the corresponding Mo_2Cl_x complexes, x = 2–10, as the number of complexed Cl is increased, are investigated to add physical insight into the nature of the sextuple bond and its dissociation energy.

The implicit inclusion of relativistic effects with pseudopotential basis sets compared to the explicit inclusion of scalar effects (momentum–velocity and Darwin corrections) via the Douglas–Kroll decoupling method up to the ninth order gives very similar $D_e(D_0)$, ω_e, and r_e values.

The inclusion of $4s^24p^6$ in the correlated space leads to a shrinkage of the calculated bond length of 0.009 Å, but the most important effect of this inclusion is that the dissociation energy is increased significantly, i.e., by 0.74 eV, which is an increase of 21% of dissociation energy of the X state. Thus, the $4s^24p^6$ electrons can be regarded as semi-valence electrons. The CBS extrapolated C-RCCSD[T] value is about 28% larger than the MRCISD+Q value. Adding this % in the MRCISD+Q D_e values of the excited states, our final D_e values are obtained (see Fig. 9). This increase agrees with our CBS limit for the $^{13}\Sigma_g^+$ state of Mo_2.

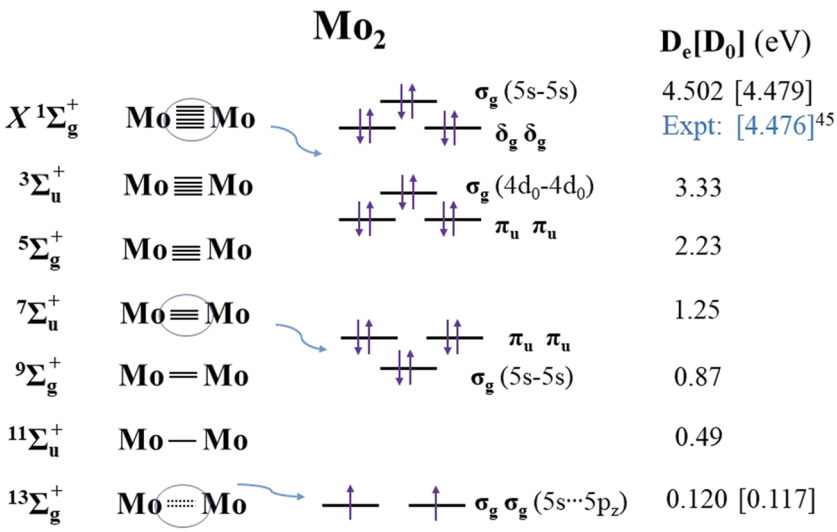

FIG. 9. Chemical bonds and dissociation energies of the $X^1\Sigma_g^+$, $^3\Sigma_u^+$, $^5\Sigma_g^+$, $^7\Sigma_u^+$, $^9\Sigma_g^+$, $^{11}\Sigma_u^+$, and $^{13}\Sigma_g^+$ states of Mo_2.

The ground state has a sextuple chemical bond and each excited state correlated with atomic ground state products has one less bond than the previous state, i.e., the triplet state has five bonds, the quintet four bonds, the septet three bonds, the nonet two bonds, and the undecet one bond, while the $^{13}\Sigma_g^+$ state is a weakly bound dimer due to two weak interactions between $5s^1\cdots5p_z{}^0$ from one Mo atom to the other one (see Fig. 9). All calculated excited states (except for the 2S + 1 = 13) have a highly multireference character, and the coefficient of the main CSF of the septet and nonet state is less than 0.3.

Regarding the bonding in the ground state, the molecular bonding orbitals can be categorized into two groups, "shells," which differ in energy by about 3 eV. The quite low bond dissociation energy of the ground state as compared to its relatively small bond length and sextuple bond ordering can be partially explained by its shell-like structure. The molecular orbital energies do not lay out evenly, and thus, the two shells are formed. Although this contributes to a strong bond with a short bond length, it also destabilizes the HOMO $2\sigma_g$ orbital, and consequently, the bond dissociation energy is relatively low.

The main electronic configuration of the X state is $\left|\pi_u^4 1\sigma_g^2 \delta_g^4 2\sigma_g^2\right\rangle$ in energetic ordering of the molecular orbitals. The $1\sigma_g{}^2$ orbital corresponds to a $(4d_{z2}–4d_{z2})^2$ bond, while the $2\sigma_g{}^2$ orbital corresponds to a $(5s–5s)^2$ bond. This ordering is maintained in the triplet and quintet states. In the septet state, the $1\sigma_g$ molecular orbital becomes the strongest molecular orbital in energy but with a different character, i.e., it is a $(5s–5s)^2$ bond. This occurs for the states with 2S + 1 = 7–11 and it results in a discontinuity at the calculated r_e, D_e, and ω_e of the septet state compared to the states with 2S + 1 = 1, 3, and 5. This change also is reflected in the change in energy separation $\Delta_{S,S-1}$ of the seven calculated states of Mo_2.

For the ground state, the calculated r_e, D_e, D_0, ω_e, and $\omega_e\chi_e$ values have been extrapolated to CBS limits via four extrapolation formulas. The CBS limits of r_e differ slightly up to 0.001 Å and the D_e values up to 0.08 eV. Our final values are r_e = 1.9324 Å and D_e (D_0) = 4.502 ± 0.007(4.471 ± 0.009) eV, which are in excellent agreement with the experimental ones of r_e = 1.929,[42] 1.938(9)[44] Å and D_0 = 4.476(10) eV.[45]

The $^{13}\Sigma_g^+$ state has a binding energy of D_e = 0.120 eV (971 cm^{-1}). Two $5s^1\cdots5p_z{}^0$ bond interactions are formed with an energy of 486 cm^{-1} at r_e = 3.53 Å resulting to a weakly bound dimer. This state resembles the six lowest energy states of Mn_2 ($X^1\Sigma_g^+$, $^3\Sigma_u^+$, $^5\Sigma_g^+$, $^7\Sigma_u^+$, $^9\Sigma_g^+$, and $^{11}\Sigma_u^+$, and $^{13}\Sigma_g^+$),[86] which are in essence degenerate packed within an energy interval of about 70 cm^{-1}. The ground state being a singlet, $X^1\Sigma_g^+$, with binding energy De (D_0) about 600(550) cm^{-1} at r_e = 3.60 Å. Here, the $^{13}\Sigma_g^+$ state of Mo_2 has almost double the binding energy at the same bond distance compared to the $^{1,3,5,7,9,11}\Sigma^+$ states of Mn_2.

Finally, all seven calculated states are part of the Mo_2Cl_x complexes, x = 2–10. For x = 2, 4, 6, and 8, the complexes are the result of covalent bond formation between the chlorines and the excited states of Mo_2 with 2S + 1 = 3, 5, 7, and 9, respectively. Thus, each pair of chlorines is bonded with a state of higher spin multiplicity. For the Mo_2Cl_{10} complex, the formation of five equivalent covalent bonds with Cl, with a Mo–Mo distance similar to this of the $^{13}\Sigma_g^+$ state of Mo_2, is not possible due to the structural constraints resulting from the size of Cl and the Mo–Mo distance. Thus, the bonding interpretation via the atomic states of the products is that: each Mo forms five covalent bonds with five Cl atoms, a weak σ ($5s^{\downarrow}–5s^{\uparrow}$) bond is formed between the two Mo atoms, and dative stabilized interactions $5p^0 \leftarrow 3p^2$ between Mo and the Cl atom that forms a covalent bond with the other Mo atom. However, even though there are additional interactions, each Mo forms six bonds, and this picture of bonding is observed in its complexes.

SUPPLEMENTARY MATERIAL

The supplementary material includes main CSFs, geometries, energetics, frequencies, and molecular orbitals of calculated states of Mo_2 and Mo_2Cl_x.

ACKNOWLEDGMENTS

The authors declare no competing financial interest.

AUTHOR DECLARATIONS

Conflict of Interest

The authors have no conflicts to disclose.

Author Contributions

Teo Depastas: Data curation (lead); Formal analysis (equal); Investigation (equal); Visualization (equal); Writing – original draft (supporting). **Alexandros Androutsopoulos:** Data curation (supporting); Formal analysis (supporting); Investigation (equal); Visualization (supporting). **Demeter Tzeli:** Conceptualization (lead); Formal analysis (equal); Investigation (equal); Methodology (lead); Project administration (lead); Resources (lead); Software (lead); Supervision (lead); Visualization (equal); Writing – original draft (lead); Writing – review & editing (lead).

DATA AVAILABILITY

The data that support the findings of this study are available within the article and its supplementary material.

REFERENCES

[1] G. N. Lewis, J. Am. Chem. Soc. **38**, 762 (1916).
[2] C. A. Coulson, Rev. Mod. Phys. **32**, 170–177 (1960).
[3] L. Pauling, *The Nature of the Chemical Bond*, 3rd ed. (Cornell University Press, Ithaca, NY, 1960), Chap. 1.
[4] G. Frenking and N. Fröhlich, Chem. Rev. **100**, 717–774 (2000).
[5] L. Zhao, S. Pan, N. Holzmann, P. Schwerdtfeger, and G. Frenking, Chem. Rev. **119**, 8781–8845 (2019).
[6] M. W. Schmidt, J. Ivanic, and K. Ruedenberg, "The physical origin of covalent bonding," in *The Chemical Bond: Fundamental Aspects of Chemical Bonding*, edited by G. Frenking and S. Shaik (Wiley-VCH Verlag GmbH & Co. KGaA, 2014), Chap. 1, pp. 1–67.
[7] A. C. West, M. W. Schmidt, M. S. Gordon, and K. Ruedenberg, J. Phys. Chem. A **119**, 10376–10389 (2015).
[8] M. W. Schmidt, J. Ivanic, and K. Ruedenberg, J. Chem. Phys. **140**, 204104 (2014).
[9] K. Ruedenberg, Rev. Mod. Phys. **34**, 326 (1962).
[10] C. Edmiston and K. Ruedenberg, J. Phys. Chem. **68**, 1628 (1964).
[11] R. R. Rue and K. Ruedenberg, J. Phys. Chem. **68**, 1676 (1964).
[12] M. J. Feinberg, K. Ruedenberg, and E. L. Mehler, Adv. Quantum Chem. **5**, 27 (1970).

[13]M. J. Feinberg and K. Ruedenberg, J. Chem. Phys. **54**, 1495 (1971); **55**, 5804 (1971).
[14]W. H. E. Schwarz, P. Valtazanos, and K. Ruedenberg, Theor. Chim. Acta **68**, 471–506 (1985).
[15]W. H. E. Schwarz, K. Ruedenberg, L. Mensching, L. L. Miller, P. Valtazanos, and W. von Niessen, Angew. Chem., Int. Ed. **28**, 597–600 (1989).
[16]K. Ruedenberg and M. W. Schmidt, J. Comput. Chem. **28**, 391–410 (2006).
[17]T. Bitter, K. Ruedenberg, and W. H. E. Schwarz, J. Comput. Chem. **28**, 411–422 (2006).
[18]K. Ruedenberg and M. W. Schmidt, J. Phys. Chem. A **113**, 1954–1968 (2009).
[19]T. Bitter, S. G. Wang, K. Ruedenberg, and W. H. E. Schwarz, Theor. Chem. Acc. **127**, 237–257 (2010).
[20]G. B. Bacskay, S. Nordholm, and K. Ruedenberg, J. Phys. Chem. A **122**, 7880–7893 (2018).
[21]G. Schoendorff, M. W. Schmidt, K. Ruedenberg, and M. S. Gordon, J. Phys. Chem. A **123**, 5249–5256 (2019).
[22]G. Schoendorff, K. Ruedenberg, and M. S. Gordon, J. Phys. Chem. A **125**, 4836–4846 (2021).
[23]H. M. Leicester, "Alexander Mikhaĭlovich Butlerov," J. Chem. Educ. **17**, 203–209 (1940).
[24]F. A. Cotton and C. B. Harris, Inorg. Chem. **4**, 330 (1965); L. Gagliardi and B. O. Roos, *ibid.* **42**, 1599–1603 (2003).
[25]S. Shaik, D. Danovich, W. Wu, P. Su, H. S. Rzepa, and P. C. Hiberty, Nat. Chem. **4**, 195–200 (2012).
[26]J. Grunenberg, Nat. Chem. **4**, 154–155 (2012).
[27]S. Shaik, H. S. Rzepa, and R. Hoffmann, Angew. Chem., Int. Ed. **52**, 3020–3033 (2013).
[28]D. Danovich, P. C. Hiberty, W. Wu, H. S. Rzepa, and S. Shaik, Chem. Eur. J. **20**, 6220–6232 (2014).
[29]L. T. Xu and T. H. Dunning, J. Chem. Theory Comput. **10**, 195–201 (2014).
[30]M. Hermann and G. Frenking, Chem. Eur. J. **22**, 4100–4108 (2016).
[31]S. Shaik, D. Danovich, B. Braida, and P. C. Hiberty, Chem. Eur. J. **22**, 4116–4128 (2016).
[32]D. W. O. de Sousa and M. A. C. Nascimento, J. Chem. Theory Comput. **12**, 2234–2241 (2016).
[33]L. F. Cheung, T.-T. Chen, G. S. Kocheril, W.-J. Chen, J. Czekner, and L.-S. Wang, J. Phys. Chem. Lett. **11**, 659–663 (2020).
[34]D. Tzeli and I. Karapetsas, J. Phys. Chem. A **124**, 6667 (2020).
[35]D. Tzeli, J. Comput. Chem. **42**, 1126–1137 (2021).
[36]T. Nguyen, A. D. Sutton, M. Brynda, J. C. Fettinger, G. J. Long, and P. P. Power, Science **310**, 844–847 (2005).
[37]B. O. Roos, A. C. Borin, and L. Gagliardi, Angew. Chem., Int. Ed. **46**, 1469–1472 (2007).
[38]D. J. Matthew, S. H. Oh, A. Sevy, and M. D. Morse, J. Chem. Phys. **144**, 214306 (2016).
[39]G. A. Ozin and W. Klotzbücher, J. Mol. Catal. **3**, 195–206 (1977).
[40]W. Klotzbücher, G. A. Ozin, J. G. Norman, Jr., and H. J. Kolari, Inorg. Chem. **16**, 2871 (1977).
[41]S. K. Gupta, R. M. Atkins, and K. A. Gingerich, Inorg. Chem. **17**, 3211 (1978).
[42]Y. M. Efremov, A. N. Samoilova, V. B. Kozhukhovsky, and L. V. Gurvich, J. Mol. Spectrosc. **73**, 430–440 (1978).
[43]M. J. Pellin, T. Foosnaes, and D. M. Gruen, J. Chem. Phys. **74**, 5547 (1981).
[44]J. B. Hopkins, P. R. R. Langridge-Smith, M. D. Morse, and R. E. Smalley, J. Chem. Phys. **78**, 1627 (1983).
[45]B. Simard, M.-A. Lebeault-Dorget, A. Marijnissen, and J. J. ter Meulen, J. Chem. Phys. **108**, 9668 (1998).
[46]D. Kraus, M. Lorenz, and V. E. Bondybey, PhysChemComm **4**, 4–48 (2001).
[47]L. A. Heimbrook, M. Rasanen, and V. E. Bondybey, J. Phys. Chem. **91**, 2468–2474 (1987).
[48]C. Wood, M. Doran, I. H. Hillier, and M. F. Guest, Faraday Symp. Chem. Soc. **14**, 159–169 (1980).
[49]J. G. Norman and P. B. Ryan, J. Comput. Chem. **1**, 59–63 (1980).
[50]B. E. Burstean and F. A. Cotton, Faraday Symp. Chem. Soc. **14**, 180–193 (1980).
[51]M. M. Goodgame and W. A. Goddard III, Phys. Rev. Lett. **48**, 135 (1982).
[52]P. M. Atha, I. H. Hillier, and M. F. Guest, Chem. Phys. Lett. **75**, 84–86 (1980).
[53]P. M. Atha and I. H. Hillier, Mol. Phys. **45**, 285–293 (1982).
[54]M. Castro, J. Keller, and P. Mareca, Int. J. Quantum Chem. **20**, 429–435 (1981).
[55]W. von Niessen, J. Chem. Phys. **85**, 337 (1986).
[56]E. A. Boudreaux and E. Baxter, Int. J. Quantum Chem. **102**, 866–868 (2005).
[57]S. Lee, D. M. Bylander, and L. Kleinman, Phys. Rev. B **37**, 10035 (1988).
[58]L. Xue-Ling, Chin. Phys. B **19**, 107103 (2010).
[59]Y.-L. Wang, H.-S. Hu, W.-L. Li, F. Wei, and J. Li, J. Am. Chem. Soc. **138**, 1126–1129 (2016).
[60]W. Zhang, X. Ran, H. Zhao, and L. Wang, J. Chem. Phys. **121**, 7717 (2004).
[61]J. Joy and E. D. Jemmis, Chem. Commun. **53**, 8168 (2017).
[62]Y. Chen, J.-y. Hasegawa, K. Yamaguchi, and S. Sakaki, Phys. Chem. Chem. Phys. **19**, 14947 (2017).
[63]R. Pis Diez and J. A. Alonso, J. Chem. Phys. **123**, 134313 (2005).
[64]F. Ruipérez, M. Piris, J. M. Ugalde, and J. M. Matxain, Phys. Chem. Chem. Phys. **15**, 2055 (2013).
[65]C. Angeli, A. Cavallini, and R. Cimiraglia, J. Chem. Phys. **127**, 074306 (2007).
[66]A. H. Kulahlioglu and L. Mitas, Comput. Theor. Chem. **1170**, 112642 (2019).
[67]R. A. Kok and M. B. Hall, Inorg. Chem. **22**, 728 (1983).
[68]F. A. Cotton, J. Mol. Spectrosc. **59**, 97–108 (1980).
[69]S.-C. Liu, W.-L. Ke, J.-S. K. Yu, T.-S. Kuo, and Y.-C. Tsai, Angew. Chem., Int. Ed. **51**, 6394 (2012).
[70]T. Chen and T. A. Manz, RSC Adv. **9**, 17072–17092 (2019).
[71]R. Haque, M. Pelino, and K. A. Gingerich, J. Chem. Phys. **71**, 2929–2933 (1979).
[72]K. A. Peterson, D. Figgen, M. Dolg, and H. Stoll, J. Chem. Phys. **126**, 124101 (2007).
[73]M. Douglas and N. M. Kroll, Ann. Phys. **82**, 89 (1974); B. A. Hess, Phys. Rev. A **32**, 756 (1985); **33**, 3742 (1986); G. Jansen and B. A. Hess, *ibid.* **39**, 6016 (1989).
[74]H. J. Werner and P. J. Knowles, J. Chem. Phys. **89**, 5803–5814 (1988).
[75]S. R. Langhoff and E. R. Davidson, Int. J. Quantum Chem. **8**, 61–72 (1974).
[76]P. J. Knowles, C. Hampel, and H. J. Werner, J. Chem. Phys. **99**, 5219–5227 (1993).
[77]D. Tzeli, I. Karapetsas, D. M. Merriles, J. C. Ewigleben, and M. D. Morse, J. Phys. Chem. A **126**, 1168–1181 (2022).
[78]S. N. Khan and E. Miliordos, J. Phys. Chem. A **123**, 5590–5599 (2019).
[79]J. Tao, J. P. Perdew, V. N. Staroverov, and G. E. Scuseria, Phys. Rev. Lett. **91**, 146401 (2003).
[80]P. J. Knowles, G. Knizia, F. R. Manby, M. Schütz, P. Celani, W. Györffy, D. Kats, T. Korona, R. Lindh *et al.*, MOLPRO 2015.1 is a package of *ab initio* programs written by H.-J. Werner.
[81]M. J. Frisch, G. W. Trucks, H. B. Schlegel, G. E. Scuseria, M. A. Robb, J. R. Cheeseman, G. Scalmani, V. Barone, G. A. Petersson, H. Nakatsuji, X. Li, M. Caricato, A. V. Marenich, J. Bloino, B. G. Janesko, R. Gomperts, B. Mennucci, H. P. Hratchian, J. V. Ortiz, A. F. Izmaylov, J. L. Sonnenberg, D. Williams-Young, F. Ding, F. Lipparini, F. Egidi, J. Goings, B. Peng, A. Petrone, T. Henderson, D. Ranasinghe, V. G. Zakrzewski, J. Gao, N. Rega, G. Zheng, W. Liang, M. Hada, M. Ehara, K. Toyota, R. Fukuda, J. Hasegawa, M. Ishida, T. Nakajima, Y. Honda, O. Kitao, H. Nakai, T. Vreven, K. Throssell, J. A. Montgomery, Jr., J. E. Peralta, F. Ogliaro, M. J. Bearpark, J. J. Heyd, E. N. Brothers, K. N. Kudin, V. N. Staroverov, T. A. Keith, R. Kobayashi, J. Normand, K. Raghavachari, A. P. Rendell, J. C. Burant, S. S. Iyengar, J. Tomasi, M. Cossi, J. M. Millam, M. Klene, C. Adamo, R. Cammi, J. W. Ochterski, R. L. Martin, K. Morokuma, O. Farkas, J. B. Foresman, and D. J. Fox, Gaussian 16, Revision C.01, Gaussian, Inc., Wallingford, CT, 2016.
[82]K. A. Peterson, D. E. Woon, and T. H. Dunning, J. Chem. Phys. **100**, 7410–7415 (1994).
[83]D. Tzeli, A. Mavridis, and S. S. Xantheas, J. Chem. Phys. **112**, 6178–6189 (2000).
[84]D. Feller, J. Chem. Phys. **138**, 074103 (2013).
[85]I. R. Ariyarathna and E. Miliordos, J. Phys. Chem. A **124**, 9783–9792 (2020).
[86]D. Tzeli, U. Miranda, I. G. Kaplan, and A. Mavridis, J. Chem. Phys. **129**, 154310 (2008).
[87]J. Beck and F. Wolf, Acta Crystallogr., Sect. B **53**, 895–903 (1997).
[88]A. Bino and F. A. Cotton, Inorg. Chem. **18**, 1381 (1979).